Appl Phys B (2009) 97: 553–560
DOI 10.1007/s00340-009-3630-9

Applied Physics B
Lasers and Optics

Characterization of an optical frequency comb using modified direct frequency comb spectroscopy

D. Aumiler · T. Ban · N. Vujičić · S. Vdović · H. Skenderović · G. Pichler

Received: 2 March 2009 / Revised version: 8 June 2009 / Published online: 27 June 2009

Abstract We introduce a method for determination of the absolute frequencies of comb lines within an optical frequency comb spectrum. The method utilizes the experimental and theoretical approach of the velocity-selective optical pumping of the atomic ground state hyperfine levels induced by resonant pulse-train excitation. The information on the laser pulse repetition frequency and carrier–envelope offset are physically mapped onto the ^{87}Rb ground state hyperfine level population velocity distributions. Theoretical spectra are calculated using an iterative analytic solution of the optical Bloch equations describing the resonant pulse-train excitation of four-level ^{87}Rb atoms. They are employed to fit the measured spectra and obtain the parameters of the frequency comb, thus providing a practical algorithm which can be used in real-time measurements.

PACS 32.80.Qk · 42.50.Gy

1 Introduction

The introduction of mode-locked femtosecond (fs) lasers in the field of optical frequency metrology offers immense resolution and precision and the highest accuracy for physical measurement [1, 2]. Due to their wide-bandwidth optical comb spectrum, today it is possible to transfer the stability of the highest-quality optical frequency standards across vast frequency gaps to other optical spectral regions or even down to the rf domain [3].

D. Aumiler · T. Ban (✉) · N. Vujičić · S. Vdović · H. Skenderović · G. Pichler
Institute of Physics, Bijenička cesta 46, Zagreb, Croatia
e-mail: ticijana@ifs.hr

Femtosecond mode-locked lasers generate ultra-short pulses by establishing a fixed phase relationship between all the lasing longitudinal modes. The laser output is characterized by a train of identical pulses, separated by a fixed time interval. The corresponding frequency spectrum of a mode-locked laser consists of a discrete, regularly spaced series of sharp lines, known as the frequency comb [4, 5]. The optical frequencies ν_n of the comb lines can be written as

$$\nu_n = nf_{\text{rep}} + f_0, \tag{1}$$

where n is a large integer of order 10^6 that indexes the comb lines, f_{rep} is the laser repetition rate and f_0 is the comb offset due to the pulse-to-pulse phase shift. This strictly regular arrangement of the comb modes across the frequency comb [6–9] with every line stable at or below the 1-Hz level is the most important feature used for optical frequency measurement and stable frequency synthesizer for both rf and optical spectral domains.

As seen in (1), determining the absolute optical frequencies of the frequency comb requires two rf frequencies, i.e. f_{rep} and f_0. While f_{rep} may be simply measured by a fast photodiode anywhere in the output beam of the fs laser, the comb offset f_0 is not determined that simply unless one has an octave-spanning frequency comb. In that case the highest frequencies of the frequency comb are a factor of two larger than the lowest frequencies. If one uses a second-harmonic crystal to frequency double a comb line from the low-frequency portion of the spectrum, it will have approximately the same frequency as the comb line on the high-frequency side of the spectrum. Measuring the heterodyne beat between these two yields a difference frequency which is equal to the offset frequency f_0. This scheme is usually

designated as self-referencing [7, 10], as it only uses the output of the fs mode-locked laser. Another scheme for the f_0 determination uses the octave-spanning comb and a cw optical standard. The cw fundamental frequency and its second harmonic are mixed with the nth comb line and its second harmonic, the $2n$th comb line. Heterodyne beats between the cw laser frequency and a comb-line frequency lying in the low- and high-frequency portions of the spectrum are measured. By mixing the beats with appropriate weighting factors the offset frequency f_0 is obtained. Most commonly, an octave-spanning spectrum is attained by coupling the output of a Ti:sapphire laser oscillator into a microstructured fibre. Although such fibers can easily broaden the femtosecond laser spectrum to greater than an octave, they also have some limitations. The breakthrough in this area was the generation of an octave-spanning spectrum directly from a femtosecond laser [11]. However, the octave-spanning spectrum is not the only way to measure f_0. Generally, by using more complicated techniques self-referencing works for any combination of two different harmonics of the same comb (for example, a self-referencing scheme that utilizes two-thirds of an octave) [12, 13].

Since mode locking is a frequency-domain concept, nowadays mode-locked lasers and their applications are typically discussed in the frequency domain. This includes optical metrology and frequency synthesis in which mode-locked lasers serve only as a simple frequency ruler. However, due to their inherent phase stability and wide-bandwidth spectrum, mode-locked lasers have started to play an important role in precision atomic and molecular spectroscopy. J. Ye's group at JILA [14, 15] developed a direct frequency comb spectroscopy (DFCS) approach which bridges the fields of high-resolution spectroscopy and ultrafast science. It uses a frequency comb for direct excitation of an atomic system and studies the time-dependent quantum coherence. This unification of the time- and frequency-domain treatments is based on the coherence accumulation effects in systems characterized by relaxation times longer than the laser repetition period. Following the time-domain approach, accumulation effects in two- and three-level rubidium atoms were investigated both experimentally and theoretically [16–18].

In our recent papers [19, 20] we have developed a modified DFCS method which utilizes a fixed-frequency comb for excitation of the rubidium atoms and an additional cw laser for probing the interaction. We have shown that resonant excitation of the room-temperature rubidium atoms by a discrete frequency comb optical spectrum results in the comb-like velocity distribution of the excited state hyperfine level populations and velocity-selective population transfer between the Rb ground state hyperfine levels. The effect is observed as strong modulations in the profiles of $5S_{1/2} \rightarrow 5P_{3/2}$ hyperfine absorption lines measured by the probe laser. The experimental results were verified by a detailed theoretical investigation of Rb multi-level atoms excited by a train of fs pulses. The generality of the observed phenomenon and the theoretical model used was confirmed by investigating the analogous effect in cesium atoms [21]. In [22] we have developed an enhanced sensitivity modified DFCS method to study the destruction of the accumulation effects. We have shown that accumulation of population and coherence, as a direct result of the frequency comb excitation, can be effectively reduced and eventually destroyed by increasing the cw probe laser intensity. Theoretical results derived from a density-matrix-based theoretical model of the eight-level Rb atoms interacting with the fs and probe laser fields showed excellent agreement with the experimental results. In order to circumvent the use of time-consuming numerical procedures and introduce an enhanced sensitivity modified DFCS method as a practical tool, we presented in our very recent paper an iterative analytic solution to the optical Bloch equations describing the fs pulse-train resonant excitation of four-level ^{87}Rb atoms [23].

In this work we employ an enhanced sensitivity modified DFCS method in conjunction with the analytic solution of the optical Bloch equations to introduce a method for the characterization of the frequency comb spectrum. We exploit the effect of velocity-selective optical pumping induced by frequency comb excitation of the room-temperature Rb atoms [19]. Since the optical pumping process is dependent upon hyperfine energy level splittings and the relative transition dipole moments, mapping of the frequency comb spectrum onto the velocity distribution of hyperfine level populations is not straightforward, and a full time-dependent theoretical modeling of the atom–laser field interaction is needed [20]. On the other hand, the theoretical modeling provides not only a qualitative but also a quantitative description of the interacting atom–laser system, as has been illustrated by the excellent agreement with the experimental results [20, 22]. Based on this agreement, using the experimentally well-known system of room-temperature Rb atoms as 'detectors' for the frequency comb, we developed a method for the determination and the monitoring of the comb-line absolute frequencies. The method is based on fitting the experimentally observed modulations in the transmission profiles of the probe laser to the theoretical model results. Since the theoretical results are derived from the analytical solution [23], we introduce this method as a simple and practical tool for the comb-frequency calibration in real time.

2 Experiment

The experimental arrangement used (see Fig. 1) is based on the modified direct frequency comb spectroscopy setup

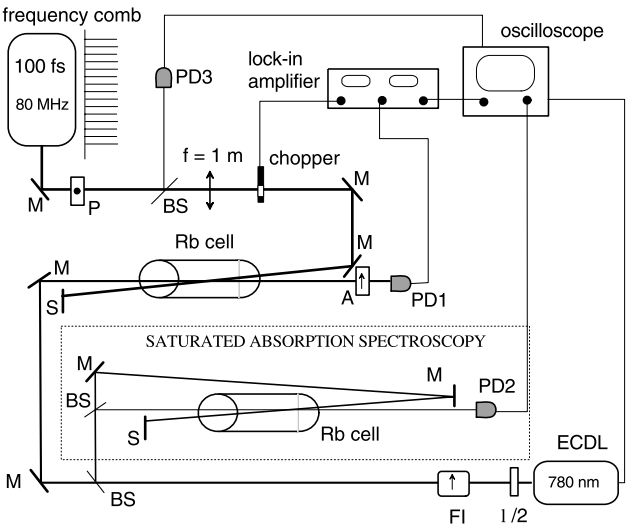

Fig. 1 Experimental scheme. PD—photodiode, P—polarizer, A—analyzer, FI—Faraday isolator, S—beam stopper

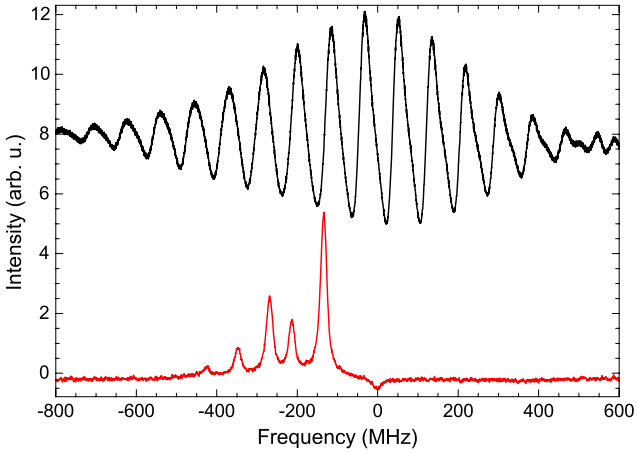

Fig. 2 Measured change in the ^{87}Rb D_2 $5S_{1/2}$ $(F = 2) \rightarrow 5P_{3/2}$ $(F = 1, 2, 3)$ probe laser transmission (780 nm) induced by the ^{87}Rb D_1 $5S_{1/2} \rightarrow 5P_{1/2}$ (795 nm) frequency comb excitation (*black line*). The saturated absorption spectrum is measured in the same probe laser scan to enable the absolute frequency calibration (*red line*)

introduced in our recent paper [22]. A Spectra Physics Tsunami mode-locked Ti:sapphire laser with pulse duration of ≈100 fs generates a ≈5.8 THz broad optical frequency comb centered at 795 nm. It uses a rf synthesizer for active mode locking by the use of an acousto-optic modulator. Besides this, the laser was not locked to any stable frequency reference, meaning that no active stabilization of the laser repetition rate f_{rep} and the carrier–envelope offset frequency f_0 was performed. Nevertheless, since the measured spectra are taken on a time scale of less than 1 s, f_{rep} and f_0 can be taken as constants during the measurement. The pulse repetition rate $f_{\mathrm{rep}} = 80.603$ MHz was measured with a fast photodiode (Thorlabs DET210, denoted by PD3 in Fig. 1).

The fs laser beam, chopped at 3.5 kHz, was weakly focused into the center of the glass cell containing room-temperature rubidium vapor. Induced changes in the ^{87}Rb $5S_{1/2}$ $(F = 2)$ ground state hyperfine level population were monitored with the cw diode laser (Toptica DL100, ECDL (External Cavity Laser Diode) at 780 nm), which propagated anticollinearly with the fs laser, intersecting it under a small angle in the center of the cell. The probe laser frequency was scanned across the Doppler-broadened ^{87}Rb D_2 $5S_{1/2}$ $(F = 2) \rightarrow 5P_{3/2}$ $(F = 1, 2, 3)$ hyperfine transitions at 3-GHz/s scanning rate. A part of the probe laser beam was used for ^{87}Rb saturated absorption spectroscopy, which was measured simultaneously with the fs laser induced changes in probe transmission, and enabled for absolute frequency calibration of the measured spectra (hyperfine splittings of the ^{87}Rb $5P_{3/2}$ state were taken from [24]).

The signal from the photodiode PD1 was fed to a Stanford Research SR510 lock-in amplifier referenced to the mechanical chopper of the fs laser beam. The lock-in signal represents the change of the probe laser transmission induced by the resonant fs pulse-train excitation of ^{87}Rb atoms. It is given by $\Delta T = T_{\mathrm{fs}} - T$, where T_{fs} and T are the probe laser transmission with and without the fs laser excitation, respectively. The measured ΔT with the corresponding saturated absorption spectrum are shown in Fig. 2.

3 Theory

The energy scheme relevant for the experiment is given in Fig. 3. Since the probe laser intensity used was far below the saturation intensity for the $5S_{1/2} \rightarrow 5P_{3/2}$ transition, the influence of the probe laser on the ground levels' population dynamics is negligible [22]. Therefore, our theoretical treatment of the problem starts by considering a four-level rubidium atom under the action of the electric field $E(t)$ of the femtosecond laser. The Hamiltonian of the system is $\hat{H} = \hat{H}_0 + \hat{H}_{\mathrm{int}}$, where $\hat{H}_0$ is the Hamiltonian of the free atom and $(H_{\mathrm{int}})_{nm} = -\mu_{nm} E(t)$ represents the interaction of the atom with the pulse train. μ_{nm} is the dipole moment of the electronically allowed $(F_{\mathrm{g}} \rightarrow F_{\mathrm{g}}, F_{\mathrm{g}} \pm 1)$ transitions, calculated from [27]. The temporal evolution of the system is given by the density matrix equations of motion [28]:

$$\begin{aligned} \frac{\partial \rho_{nm}}{\partial t} &= \frac{-\mathrm{i}}{\hbar}\left[\hat{H}, \hat{\rho}\right]_{nm} - \gamma_{nm}\rho_{nm} \quad (n \neq m), \\ \frac{\partial \rho_{nn}}{\partial t} &= \frac{-\mathrm{i}}{\hbar}\left[\hat{H}, \hat{\rho}\right]_{nn} - \sum_{m(E_m < E_n)} \Gamma_{mn}\rho_{nn} \\ &\quad + \sum_{m(E_m > E_n)} \Gamma_{nm}\rho_{mm}, \end{aligned} \tag{2}$$

where the subscripts nm refer to the hyperfine levels numbered from the lowest to the highest energy level (see Fig. 3). Γ_{nm} gives the population decay rate from level m to level n

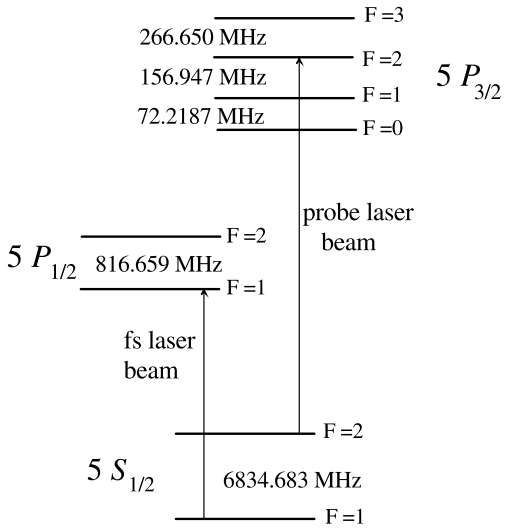

Fig. 3 ^{87}Rb D_1 and D_2 transitions. $5S_{1/2}$ ground state values are taken from [25] and $5P_{1/2}$ excited-state values are taken from [26]

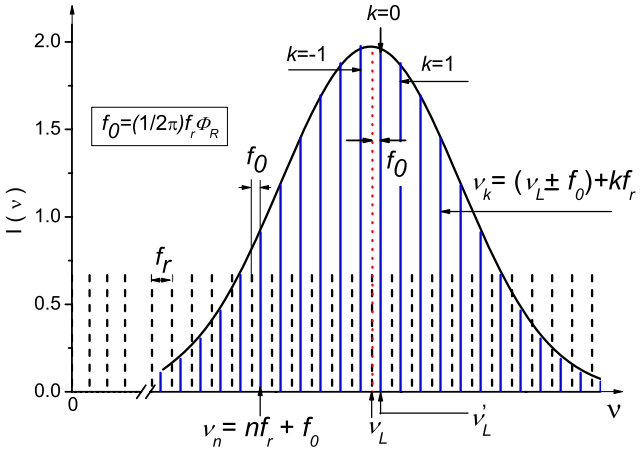

Fig. 4 Two equivalent schemes of frequency comb representation given in the frequency domain

[27], whereas γ_{nm} is the damping rate of the ρ_{nm} coherence given by

$$\gamma_{nm} = \frac{1}{2}(\Gamma_n + \Gamma_m), \tag{3}$$

where Γ_n and Γ_m denote the total population decay rates of levels n and m. The usual method for solving the system of equations (2) is to invoke the rotating-wave approximation by introducing the slowly varying envelope of the laser pulse electric field $\mathcal{E}(t) = E(t)\mathrm{e}^{-\mathrm{i}\omega_\mathrm{L}t}$ and the slowly varying envelope of the coherence $\sigma_{nm} = \rho_{nm}\mathrm{e}^{-\mathrm{i}\omega_\mathrm{L}t}$, where ω_L is the central laser frequency. The resulting set of coupled differential equations describes the temporal evolution of the slowly varying elements of the density matrix (i.e. populations and coherences) [20].

The slowly varying envelope of the pulse-train electric field is given by

$$\mathcal{E}_T(t) = \sum_{n=0}^{\infty} \mathcal{E}(t - nT_\mathrm{R})\mathrm{e}^{\mathrm{i}n\Phi_\mathrm{R}}, \tag{4}$$

where T_R is the laser repetition period and Φ_R is the round-trip phase acquired by the laser within the cavity (pulse-to-pulse phase shift). The frequency spectrum of $\mathcal{E}_T(t)$ consists of a comb of laser modes separated by $2\pi/T_\mathrm{R} = 2\pi f_\mathrm{rep}$ and centered at $\omega_\mathrm{L} + \Phi_\mathrm{R}/T_\mathrm{R}$. The kth mode frequency of the pulse-train laser field is then given by

$$\omega_k = \left(\omega_\mathrm{L} + \frac{\Phi_\mathrm{R}}{T_\mathrm{R}}\right) \pm \frac{2\pi k}{T_\mathrm{R}}. \tag{5}$$

We solved (2) by invoking the iterative analytic solution given in [23], obtained for $\Phi_\mathrm{R} = 0$. By inspection of (5), it is evident that under this simplification the absolute frequencies of the comb lines are defined by two independent parameters: the central laser frequency ω_L and the laser repetition frequency $2\pi/T_\mathrm{R}$. This simplification is reasonable since ω_L and Φ_R together define the frequency shift of the complete frequency comb spectrum, and it simply reflects our lack of experimental knowledge of both the central laser frequency and Φ_R. Additionally, it has been shown in [16, 20, 23] that, in view of the resonant frequency comb excitation of atoms, changing ω_L and Φ_R has the same effect on the atom excitation and optical pumping process, and therefore also on the resulting hyperfine level populations. Equation (5) can therefore be written as

$$\omega_k = \omega_\mathrm{L}' \pm 2\pi k f_\mathrm{rep}, \tag{6}$$

which corresponds to (1). This correspondence is schematically shown in Fig. 4. We refer to ω_L' as the central laser frequency throughout the rest of the paper and drop the prime notation for convenience. If the laser repetition period is smaller than the characteristic relaxation times of the atomic system, the atoms can never completely relax between two consecutive laser pulses. As a result, the medium accumulates excitation in the form of coherence and excited-state population. After a large number of consecutive pulses, the system reaches a stationary state (which is repeated with a period T_R) characterized by the enhanced excited state population and coherence. This enhancement is similar to the constructive interference phenomenon, since the time-delayed phases acquired by the coherence with the succession of pulses are analogous to the time-delayed phases in a multiple-slit experiment. The accumulation of population and coherence in rubidium atoms excited by the train of fs pulses was extensively studied in our previous papers [19, 20]. The inhomogeneous Doppler broadening was included by replacing atomic transition frequencies ω_{nm} with $\omega_{nm} + \vec{k}_\mathrm{fs} \cdot \vec{v}$, where $\vec{k}_\mathrm{fs}$ is the fs laser wavevector and $\vec{v}$ is the atomic velocity. In this case different velocity groups corre-

spond to different detunings, $\vec{k}_{\mathrm{fs}} \cdot \vec{v}$, from the atomic transition frequency, so different velocity groups are in different situations with respect to the excitation (accumulation) process. This leads to the velocity-selective optical pumping of ground hyperfine levels and velocity-selective population in excited hyperfine levels [19, 20]. As a result, physical mapping of the frequency comb spectra to the hyperfine population distributions is observed [19, 20].

In order to calculate the hyperfine level population distributions, one has to solve the set of equations (2) separately for each velocity group. The time evolution of the hyperfine level populations is obtained using the analytical solution given in [23] and the population values at time τ_0 are taken as the final populations [19]. The time τ_0 is given as the average time of interaction of atoms with the fs laser and is deduced from the fs laser beam cross section and the average atom velocity (in our experimental conditions, τ_0 corresponds to a sequence of $\approx$100 pulses). This is where the advantage of the analytical solution is clearly evident, since the full numerical calculation of the population velocity distributions takes several hours, while the application of the analytical solution gives the same result in less than a second.

In the experiment, the effect of the pulse-train excitation on the ground state hyperfine population distributions is monitored by the probe laser. The changes in the ground state hyperfine level population distributions (ρ_{11} and ρ_{22}) are not measured directly, but through the changes in the ^{87}Rb D$_2$ $5S_{1/2} \rightarrow 5P_{3/2}$ absorption spectra at 780 nm, induced by the frequency comb excitation. The influence of the probe laser on the ground state populations is neglected, since the probe laser intensity was far below the saturation intensity for the Rb $5S_{1/2} \rightarrow 5P_{3/2}$ transition [29]. In order to compare theory with experiment, it is therefore necessary to simulate the D$_2$ resonance line hyperfine absorption spectra using the ground state population distributions obtained by solving the density matrix equations (2). The simulation of the ^{87}Rb D$_2$ $5S_{1/2}\,(F=2) \rightarrow 5P_{3/2}\,(F=1,2,3)$ hyperfine absorption line is illustrated in Fig. 5. The line consists of three hyperfine components coming from the hyperfine splitting of the excited state. For each hyperfine component, we calculate the convolution of the velocity distribution of the ground $F=2$ hyperfine level population ρ_{22} with the Lorentzian profile of the natural line width. Pulse-train parameters used in the calculation are $\mathcal{E}_0 = 2 \times 10^6$ V/m, $\tau_{\mathrm{p}} = 100$ fs, $f_{\mathrm{rep}} = 80.7$ MHz, $\Phi_{\mathrm{R}} = 0$ and ω_{L} in resonance with the $5S_{1/2}\,(F=1) \rightarrow 5P_{1/2}\,(F=1)$ hyperfine transition. The total $5S_{1/2}\,(F=2) \rightarrow 5P_{1/2}\,(F=1,2,3)$ absorption line profile is obtained by adding the contributions of the three hyperfine components.

In the last step of the simulation procedure, the absorption line profile (with and without frequency comb excitation) is used to calculate the changes in the probe laser transmission spectra induced by the frequency comb excitation. This is achieved by the simple application of Beer–Lambert's law and, as a result, the theoretical signal is generated and can be directly compared to the measured one [22].

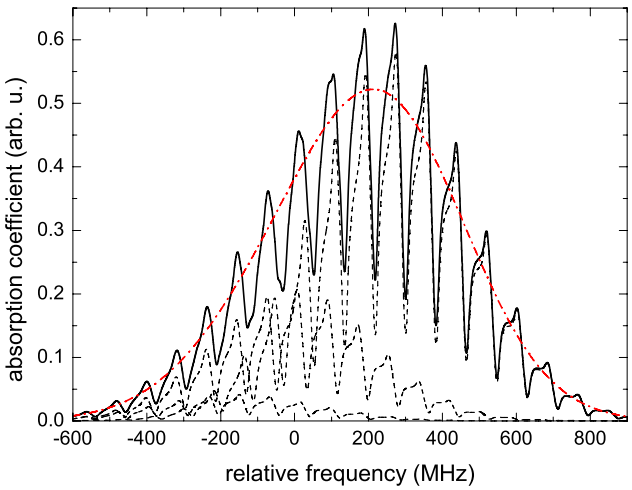

Fig. 5 Simulation of the ^{87}Rb D$_2$ $5S_{1/2}$ $(F=2) \rightarrow 5P_{3/2}$ $(F=1,2,3)$ hyperfine absorption spectra using the ground state $F=2$ level population velocity distribution ρ_{22}. Contributions of the three hyperfine components forming the line are shown (*dashed line*), together with the resulting line profile (*solid line*) and the line profile without the frequency comb excitation (*dash–dot line*)

4 Results

Typical measured and simulated signals of the change in probe laser transmission ΔT induced by the fs pulse-train excitation are shown in Fig. 6. The spectra possess a strongly pronounced oscillatory structure, with the period given by the fs laser repetition frequency, whereas the spectral envelope of the signals is given by the ^{87}Rb D$_2$ $5S_{1/2}\,(F=2) \rightarrow 5P_{3/2}\,(F=1,2,3)$ absorption line profile. Due to the Doppler broadening, which is larger than the hyperfine energy splittings of the excited $5P_{3/2}$ state, the absorption line consists of three unresolved hyperfine components of the excited state. Generally, the shape of the signal is given by the physical parameters of the ^{87}Rb atom (hyperfine energy splittings and transition dipole moments) and the fs pulse train (pulse peak power, repetition frequency and central laser frequency), as was discussed in detail in [20, 22].

Since the physical parameters of the ^{87}Rb atom are well known, one can gain relevant information about the parameters of the fs pulse train by a simple comparison of the simulated and experimental transmission spectra. If the basic physical parameters of the fs pulses are directly measured, i.e. fs laser average power, pulse repetition frequency and pulse duration, then the fs laser central frequency ω_{L} remains as the only free parameter of the pulse train that distinguishes the simulated signal from the measured one. By

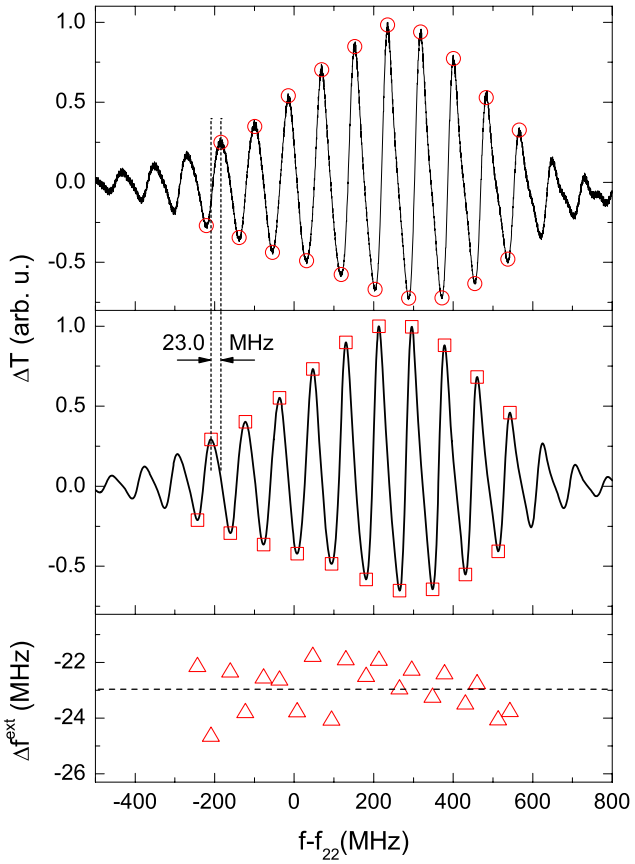

Fig. 6 Comparison of the experimental (*upper panel*) and simulated (*middle panel*) changes in the probe laser transmission induced by the frequency comb excitation. Absolute frequencies of the maxima and minima in the experimental signal (*circles*) are subtracted from the corresponding extremes in the simulated signal (*squares*) to obtain the Δf^{ext} values shown in the lower panel (*triangles*), with $\overline{\Delta f^{\mathrm{ext}}}$ indicated by a *dashed line*. The absolute frequency scale of the figure is given in terms of the ^{87}Rb D$_2$ $5S_{1/2}\,(F=2) \rightarrow 5P_{3/2}\,(F=2)$ hyperfine transition frequency f_{22}

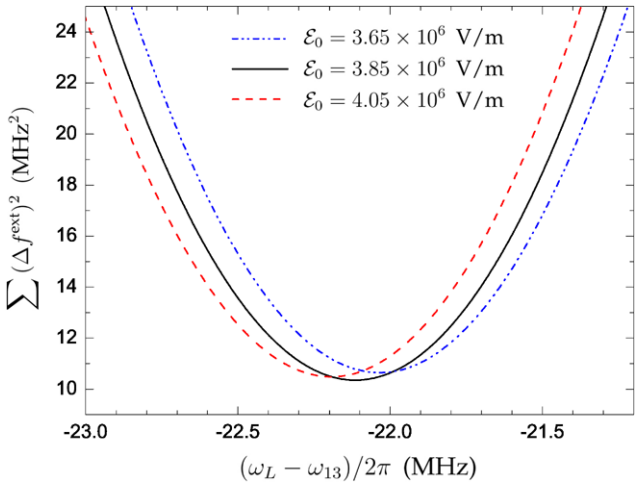

Fig. 7 Fitting of the simulated to the measured ΔT spectra with ω_{L} taken as a free parameter. The results for three different peak pulse amplitudes are shown (*solid line* corresponds to the experimental conditions); other pulse-train parameters are the same as in Fig. 6

fitting the simulated spectra to the measured spectra with ω_{L} taken as a free parameter, one can determine the central fs laser frequency. Together with the measured pulse repetition frequency f_{rep}, using (6), we can therefore determine the absolute frequencies ω_k of all comb lines of the frequency comb (and, by doing so, also the frequency comb offset frequency f_0).

The full numerical fitting procedure for overlapping the simulated and measured signals can be avoided altogether by application of the simpler procedure. One can merely determine the absolute frequencies of the maxima and minima in the measured transmission spectrum $f^{\mathrm{ext}}_{\mathrm{exp}}$ (indicated by circles in Fig. 6) and subtract them from the corresponding frequencies in the simulated spectrum $f^{\mathrm{ext}}_{\mathrm{th}}$ (squares in Fig. 6). As a result a series of points is obtained, $\Delta f^{\mathrm{ext}} = f^{\mathrm{ext}}_{\mathrm{th}} - f^{\mathrm{ext}}_{\mathrm{exp}}$, grouped around a certain mean theory–experiment frequency offset value $\overline{\Delta f^{\mathrm{ext}}}$. This frequency offset represents the frequency offset of the actual frequency comb lines with respect to the arbitrarily chosen value for ω_{L} in the simulation, and it should not be confused with the frequency comb offset frequency f_0. The procedure is illustrated in Fig. 6, where the frequency offset $\overline{\Delta f^{\mathrm{ext}}}$ of -23.0 ± 0.8 MHz was obtained for the central fs laser frequency ω_{L} set in resonance with the ^{87}Rb D$_1$ $5S_{1/2}\,(F=1) \rightarrow 5P_{1/2}\,(F=1)$ hyperfine transition ($\omega_{\mathrm{L}} = \omega_{13} = 2\pi \times 377111224.486$ MHz [25, 26]). Other pulse parameters in the simulation were $\mathcal{E}_0 = 3.85 \times 10^6$ V/m, $\tau_{\mathrm{p}} = 100$ fs and $f_{\mathrm{rep}} = 80.603$ MHz, corresponding to the experimental conditions.

Since the frequency shift of the frequency comb spectrum, together with the corresponding mapped hyperfine level population velocity distribution, is achieved by changing the fs laser central frequency, it follows that the overlap of the simulated and the measured transmission spectra should be obtained for the fs central laser frequency ω_{L} shifted from the ω_{13} resonance by –23.0 MHz. However, it should be emphasized that this value was obtained in the frequency domain of the probe laser (Doppler shift governed by the probe laser wavevector k_{p}), whereas the velocity-selective optical pumping process occurs in the domain of the fs laser (Doppler shift governed by the fs laser wavevector k_{fs}). Therefore, the obtained frequency shift value should be multiplied by the factor $k_{\mathrm{fs}}/k_{\mathrm{p}}$. The final result for the central fs laser frequency, based on the results shown in Fig. 6, is then $(\omega_{\mathrm{L}} - \omega_{13})/2\pi = -22.5 \pm 0.8$ MHz.

This result can be compared with the result obtained using the fitting procedure of the simulated ΔT signal to the measured one (Fig. 7). ω_{L} is taken as a free parameter and the fitting error is given as the sum of the squares of frequency differences between the simulated and experimental minima and maxima in the ΔT signal, $\sum (f^{\mathrm{ext}}_{\mathrm{th}} - f^{\mathrm{ext}}_{\mathrm{exp}})^2$.

As can be seen from Fig. 7, the numerical precision of the method is about 0.1 MHz. The result for the central fs laser frequency is $(\omega_L - \omega_{13})/2\pi = -22.1 \pm 0.1$ MHz, which is in agreement with the value of -22.5 ± 0.8 MHz obtained with the simplified procedure.

Since the numerical procedure and simulation results are dependent upon the measured pulse-train parameters, it is instructive to see how the uncertainty of the measured quantity (namely, the pulse peak amplitude) affects the final results for ω_L. As illustrated in Fig. 7, a 5% increase or decrease of $\mathcal{E}_0$ from the measured peak pulse amplitude value of 3.85×10^6 V/m results in the change in the fitted ω_L value which is within the numerical precision of the method of 0.1 MHz. This suggests that only a negligible change in the shape of modulations of the probe transmission profile ΔT occurs when changing $\mathcal{E}_0$ in this power range (the relative amplitude of the modulations changes, but the shape itself does not), which is in agreement with our previous observations [20].

Finally, it should be noted that the overall accuracy of the method is strongly influenced by the quality of the absolute frequency calibration based on saturation spectroscopy. In our present experimental arrangement, the accuracy of ± 0.7 MHz was achieved in the absolute frequency calibration of the probe laser scan. Additionally, we estimate the accuracy of the measured ΔT maxima/minima frequency determination to be ± 0.3 MHz. Together with the stated numerical precision of the fitting procedure of 0.1 MHz, we estimate that the overall accuracy of the presented method for frequency calibration of comb lines is about 0.8 MHz.

5 Conclusion

We have developed an alternative method for determination of the absolute frequencies of comb lines within an optical frequency comb spectrum. The method is based on velocity-selective optical pumping of atomic ground state hyperfine levels induced by resonant pulse-train excitation. The effect is observed in room-temperature atoms if the atomic relaxation times are longer than the pulse repetition period and is caused by coherence accumulation. Theoretical treatment of the effect, based on optical Bloch equations (presented in detail in [19, 20]), enables the study of the system's time dynamics and gives information on the influence of the frequency comb excitation on the ground state hyperfine level population distribution. As reported in [20], a phenomenon of physical mapping of the frequency comb to the ground state hyperfine level populations can be enlightened in this way. This mapping is strongly affected by the physical parameters of the atoms of interest (hyperfine energy splittings and relative transition moments) and also by the parameters of the frequency comb (frequencies of the comb modes). By utilizing a well-known atomic system, such as Rb atoms, the mapping can be effectively exploited to retrieve information about the frequency comb used for excitation.

A modified direct frequency comb spectroscopy method is used to experimentally observe the mapping in the case of ^{87}Rb D_1 $5S_{1/2} \rightarrow 5P_{1/2}$ (795 nm) pulse-train excitation, while the probe laser is used to monitor the ^{87}Rb $5S_{1/2}$ ($F = 2$) hyperfine level population by measuring the changes in the ^{87}Rb D_2 $5S_{1/2}(F = 2) \rightarrow 5P_{3/2}(F = 1, 2, 3)$ (780 nm) absorption. The experimental results are compared to the results of the theoretical model to characterize the frequency comb.

In order to make the method applicable in practical experiments, we used the iterative analytic solution to the optical Bloch equations describing the system of interest given in [23]. By measuring the pulse repetition frequency (as an input parameter for the model), the method reduces to the one-parameter fitting procedure for obtaining the central fs laser frequency. By fitting the simulated probe transmission signal to the measured one the central fs laser frequency is obtained, leading to the determination of the absolute frequencies of all comb lines within the optical frequency comb spectrum (see (5)).

Besides the fs laser and some basic laboratory electronics, the method only uses a Rb glass cell (which is used both as a 'detector' for the frequency comb and as a frequency reference) and a probe laser. By implementing the simulation and fitting procedure on a standard laboratory PC, the method can be used to obtain the absolute frequencies of the comb lines in real time with an accuracy of better than 1 MHz. The method does not need complex second-harmonic systems for the absolute frequency comb calibration and it could be used in experiments concerning systems influenced by thermal, pressure or electromagnetic field effects, where a resolution above 1 MHz could be expected.

We are currently working on the implementation of the same method but using a probe laser at 795 nm, which covers the ^{87}Rb D_1 transition. In that case there will be no need to compose the profile as shown in Fig. 5, since the hyperfine splitting of the $5P_{1/2}$ excited state is about 816 MHz (hyperfine absorption lines are completely resolved even at room temperature). We believe that this improvement will increase the resolution of our method below 1 MHz. In addition, the measured signal will represent direct mapping of the frequency comb to the ground state population distributions and can therefore be used as a simple marker of the frequency comb lines.

Acknowledgements We acknowledge support from the Ministry of Science, Education and Sports of the Republic of Croatia (Project No. 035-0352851-2857).

References

1. A.D. Ludlow, T. Zelevinsky, G.K. Campbell, S. Blatt, M.M. Boyd, M.H.G. de Miranda, M.J. Martin, J.W. Thomsen, S.M. Foreman, J. Ye, T.M. Fortier, J.E. Stalnaker, S.A. Diddams, Y. Le Coq, Z.W. Barber, N. Poli, N.D. Lemke, K.M. Beck, C.W. Oates, Science **319**, 1805 (2008)
2. T. Rosenband, D.B. Hume, P.O. Schmidt, C.W. Chou, A. Brusch, L. Lorini, W.H. Oskay, R.E. Drullinger, T.M. Fortier, J.E. Stalnaker, S.A. Diddams, W.C. Swann, N.R. Newbury, W.M. Itano, D.J. Wineland, J.C. Bergquist, Science **319**, 1808 (2008)
3. J.Y.S. Cundiff, J. Hall, Sci. Am. April, 74 (2008)
4. J. Ye, S.T. Cundiff, *Femtosecond Optical Frequency Comb Technology* (Springer, Boston, 2005)
5. S.T. Cundiff, J. Ye, Rev. Mod. Phys. **75**, 325 (2003)
6. T. Udem, J. Reichert, R. Holzwarth, T.W. Hänsch, Opt. Lett. **24**, 881 (1999)
7. R. Holzwarth, T. Udem, T.W. Hänsch, J.C. Knight, W.J. Wadsworth, P.S.J. Russell, Phys. Rev. Lett. **85**, 2264 (2000)
8. S.A. Diddams, L. Hollberg, L.S. Ma, L. Robertsson, Opt. Lett. **27**, 58 (2002)
9. L.S. Ma, Z. Bi, A. Bartels, L. Robertsson, M. Zucco, R.S. Windeler, G. Wilpers, C. Oates, L. Hollberg, S.A. Diddams, Science **303**, 1843 (2004)
10. S.A. Diddams, D.J. Jones, J. Ye, S.T. Cundiff, J.L. Hall, J.K. Ranka, R.S. Windeler, R. Holzwarth, T. Udem, T.W. Hänsch, Phys. Rev. Lett. **84**, 5102 (2000)
11. U. Morgner, R. Ell, G. Metzler, T.R. Schibli, F.X. Kärtner, J.G. Fujimoto, H.A. Haus, E.P. Ippen, Phys. Rev. Lett. **86**, 5462 (2001)
12. H.R. Telle, G. Steinmeyer, A.E. Dunlop, J. Stenger, D.H. Sutter, U. Keller, Appl. Phys. B, Lasers Opt. **69**, 327 (1999)
13. T.M. Ramond, S.A. Diddams, L. Hollberg, A. Bartels, Opt. Lett. **27**, 1842 (2002)
14. A. Marian, M.C. Stowe, J.R. Lawall, D. Felinto, J. Ye, Science **306**, 2063 (2004)
15. M.C. Stowe, M.J. Thorpe, A. Pe'er, J. Ye, J.E. Stalnaker, V. Gerginoo, S.A. Diddams, Adv. At. Mol. Opt. Phys. **55**, 1 (2008)
16. D. Felinto, C.A.C. Bosco, L.H. Acioli, S.S. Vianna, Opt. Commun. **215**, 69 (2003)
17. D. Felinto, L.H. Acioli, S.S. Vianna, Phys. Rev. A **70**, 043403 (2004)
18. D. Felinto, C.A.C. Bosco, L.H. Acioli, S.S. Vianna, Phys. Rev. A **64**, 063413 (2001)
19. D. Aumiler, T. Ban, H. Skenderović, G. Pichler, Phys. Rev. Lett. **95**, 233001 (2005)
20. T. Ban, D. Aumiler, H. Skenderović, G. Pichler, Phys. Rev. A **73**, 043407 (2006)
21. N. Vujičić, S. Vdović, D. Aumiler, T. Ban, H. Skenderović, G. Pichler, Eur. Phys. J. D **41**, 447 (2007)
22. T. Ban, D. Aumiler, H. Skenderović, S. Vdović, N. Vujičić, G. Pichler, Phys. Rev. A **76**, 043410 (2007)
23. D. Aumiler, T. Ban, G. Pichler, Phys. Rev. A **79**, 063403 (2009)
24. J. Ye, S. Swartz, P. Jungner, J.L. Hall, Opt. Lett. **21**, 1280 (1996)
25. S. Bize, Y. Sortais, M.S. Santos, C. Manache, A. Clarion, C. Salomon, Europhys. Lett. **45**, 558 (1999)
26. M. Maric, J.J. McFerran, A.N. Luiten, Phys. Rev. A **77**, 032502 (2008)
27. O. Axner, J. Gustafsson, N. Omenetto, J.D. Winefordner, Spectrochim. Acta Part B **59**, 1 (2004)
28. R.W. Boyd, *Nonlinear Optics* (Academic Press, San Diego, 2003)
29. D.A. Steck, Alkali D line data. http://steck.us/alkalidata